Greenhouse gas fluxes in an urban area

Alina Jasek

AGH-University of Science and Technology
Faculty of Physics and Applied Computer Science
Kraków, Poland

Kraków, Poland
24 July 2014

1. Purpose of the visit

As the urban ecosystem is recognized to be a vital element of local and global carbon cycle, it is emphasized to study mechanisms of transport and storage of carbon in this particular environment. Several stations are located within the cities around the world (including northern [1], temperate [2], Mediterranean [3] and tropical [4] sites), to measure CO_2 and CH_4 urban fluxes. Direct measurements of biogenic emissions [1, 5] and estimations of anthropogenic input of CO_2 to the local atmosphere [6] have been performed as well.

The authors' PhD work, to be finished in 2015, will be centered on a carbon balance of the city of Kraków, southern Poland, with a particular focus on a biosphere-atmosphere exchange of carbon dioxide. Several studies regarding the carbon balance in this city have been performed so far, including long record of atmospheric mixing ratios (e.g. [6]) as well as characterization of isotopic signatures of anthropogenic [7] and biogenic [5] sources. Since 2012, measurements of CO_2 and CH_4 flux from Krakow ecosystem to the atmosphere are being performed using relaxed eddy accumulation (REA) method, which is a modified version of eddy covariance (EC). A study site description can be found in **Box 1**.

Author visited Helsinki University in order to gain experience in dealing with micrometeorological measurement methods in a complex urban terrain, including footprint analysis, applicability of corrections, extensive analysis of CO_2 and CH_4 fluxes from Kraków and comparison of fluxes from Kraków and Helsinki. Secondary aim was to use the opportunity to gain knowledge of measuring aerosols in an urban area.

Box 1. Study site description.

In July 2012, measurements of CO_2 and CH_4 flux from Kraków ecosystem to the atmosphere using relaxed eddy accumulation method started. The REA site is located on the top of a Faculty of Physics and Applied Computer Science building in Kraków, surrounded by a heterogeneous terrain, which includes a park, an urban meadow, high and low traffic lanes and residential buildings **(Fig. 1b)**. For extensive Kraków study site description, see e.g. [6].

A REA method is a modification of eddy covariance that allows using a slow concentration analyzer. The air inlet and 3D anemometer are located on a top of the mast (**Fig.1a**). The anemometer checks vertical wind direction with 10Hz frequency, and according to it *updraft* or *downdraft* sampling bag is being filled. Bag filling lasts each half-hour period, and when one pair of samples is being measured with a gas analyzer, the other pair can be filled.

Gas flux can be calculated with Eq.1:

$$F = \beta \sigma_w \left(C^{up} - C^{dw} \right) \qquad \textbf{(Eq. 1)}$$

where F is a gas flux, β is an empirical constant equal to 0.56 [8], σ_w stands for vertical wind velocity standard deviation for a given half-hour period, and C^{up} and C^{dw} are gas concentrations measured in *updraft* and *downdraft* bag.

The mast is an 20m high aluminum construction, installed on a rooftop of a four-stores building **(Fig. 1a)**. Measurement height z is 39.7 m. According to the general rules of thumb, the effective measurement height z_m is equal to 26 m, and fetch is less than 2 km. Roughness length is assumed 2m for a complex urban site, following [9]. On a top of the mast a Gill Windmaster Pro (Gill Ind., Grand Rapids, MI, USA) sonic anemometer is installed as well as REA inlets and valves of *downdraft* and *updraft* sampling system. Remaining REA components, along with concentration analyzer Picarro 2101*i* (Picarro Inc., Santa Clara, CA, USA) are located in the laboratory near the mast base. A basic footprint estimation have been made using a theoretical model developed by Gash in 1986 (**Fig. 1b**, for a model description see [10]). For a given measurement height, peak footprint values were estimated around 170m, and 90% of the signal source area is within 3 km from the measurement site.

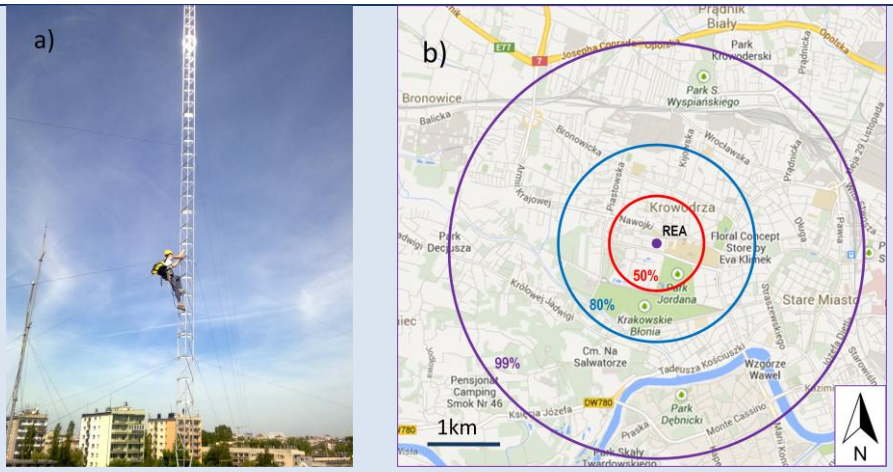

Fig. 1. a) *Photo of a REA mast located in Kraków and* ***b)*** *map of the mast surroundings with an ideal footprint estimation of analytical model [10].*

The REA system being used for CO_2 and CH_4 flux measurements is presented in **Fig. 2**. Hourly measurement schedule is deployed with two sets of sampling bags: when the first pair is being filled, the second is being measured with gas analyzer, leaving 30 minutes for direct concentration measurement.

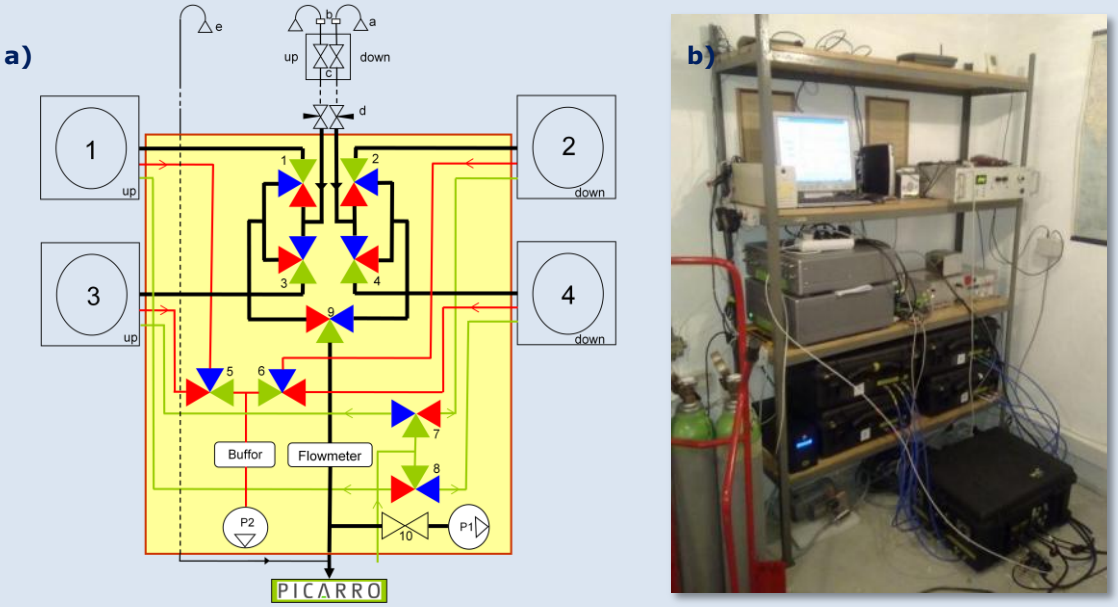

Fig. 2. *a) REA system schematics: 1-4 updraft and downdraft sampling bags, valves 1-10 control bag filling and emptying, a – air inlets, b – filters, c – fast changing valves, d – flow controllers, e – additional air inlet for direct concentration measurement; b) REA sampling system (black cases) with Picarro G2101i gas analyzer (grey boxes) in the laboratory located at AGH-UST campus.*

REA data processor (AGH-UST, 2012) calculates CO_2 and CH_4 fluxes using raw data provided by anemometer and concentration measurement from the gas analyzer. The software allows a manual quality control of concentration measurement and dispose of unreliable results. No corrections are implemented in the software so far.

2. Work description

2.1. Footprint analysis

A theoretical footprint analysis for Kraków site was performed using two independent models: Kormann and Meixner ([11], software provided by the hosting institute) and Kljun [12], in addition to basic estimation of the Gash model. Input model parameters were established using roughness length, measurement height and boundary layer height estimated for Krakow site **(Box 1)**. The site surroundings were divided into four

sectors with assumed different CO_2 source types. The results of footprint calculations are presented in Chapter 3.2.

2.2. Corrections application

As the software that have been used to flux calculations does not have the corrections implemented so far, author used EddyPro software (LiCOR Biosciences, Lincoln, Nebraska, USA) to calculate vertical wind component statistics and compare it to the uncorrected values. Data processing included raw data (*step 1*) despiking (*step 2*), cross-wind (*step 3*) and angle of attack (*step 4*) corrections, coordinates rotation (*step 5*) and linear detrending (*step 7*) (*Step 6* of correcting procedure is related to time lag compensation and therefore not applicable to this work).

Fig. 3 presents the impact of each correction on the vertical wind speed component and its variance.

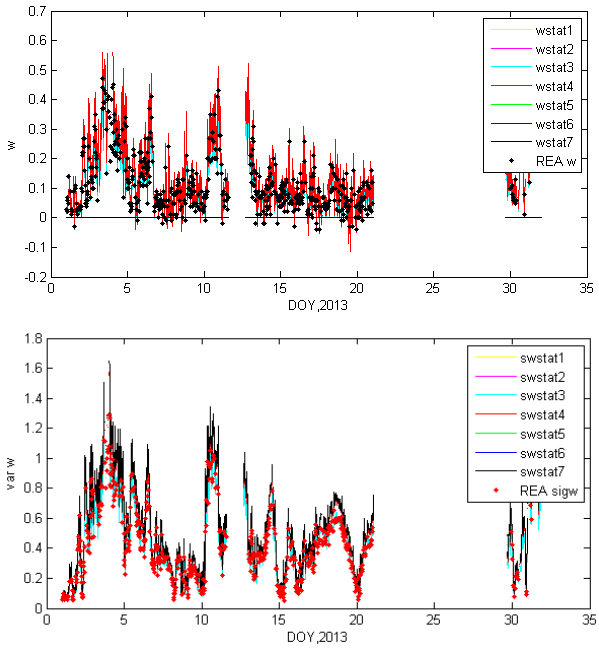

Fig. 3. *Calculated half-hourly mean values of wind vertical component* w *(top figure) and its variance (bottom figure) for January 2013. Each color represents another step in EddyPro correcting procedure, red dots are uncorrected values calculated by the REA data processor.*

Applying the corrections have an impact on the results: after the tilt correction associated with rotation of coordinates, mean *w* values naturally are very close to 0; uncorrected *w* standard deviations are around 20% lower than corrected, which lead to a serious underestimation of calculated fluxes. For a final flux calculation corrected σ_w values obtained from EddyPro were used.

A possible malfunction in the sampling system was discovered, lasting from July to December 2013. All the fluxes calculated for that period are noticeably biased towards lower values **(Fig. 4).** As no such bias is visible in the calculated standard deviations of wind vertical component **(Fig 4**, inset**)**, a most possible reason is some kind of malfunction of the sampling system causing a systematic error – for example, leaking bags. During that exact period, *updraft* and *downdraft* sampling tubes were switched, changing the sign of the calculated flux (which have already been corrected).

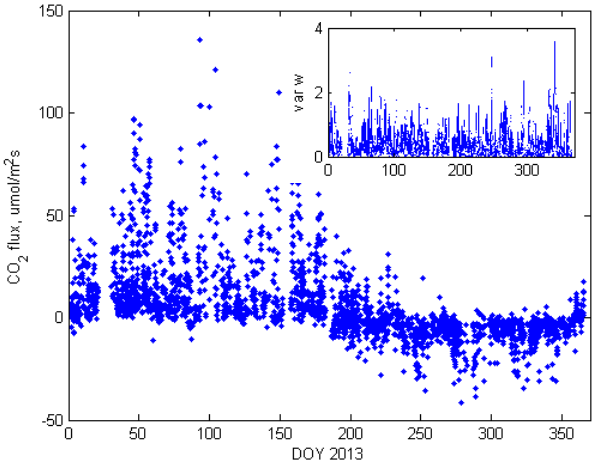

Fig. 4. *CO_2 flux in 2013 along with biased period from July to December (large plot). Variance of vertical wind component during the same period with no systematic bias (insect).*

However unrealistic wintertime fluxes (December median below zero, suggesting CO_2 assimilation) confirm the possibility of malfunctioning system, this explanation is

only a hypothesis. A thorough analysis of data record of that period is needed.

For a purpose of this report, the unreliable data period was not taken into account for the further analysis and will be discarded until explained and corrected, if possible.

2.3. Flux data analysis

Analysis of a data record from July 2012 to March 2014 from Kraków site have been made. Preliminary calculation of fluxes of CO_2 and CH_4 was performed in advance of a visit, using software created at AGH-UST (REA data processor, 2012). According to relaxed eddy accumulation principles, the gas flux is calculated by multiplying standard deviation of vertical wind velocity σ_w by a difference between concentration in *updraft* and *downdraft* samples **(Box 1)**.

Data quality control implemented in the software allowed to filter out the results which do not fulfill steady state or developed turbulent conditions test [13].

An additional comment is needed to an application of offline tilt correction for relaxed eddy accumulation. A commonly used method of implementation of coordinates rotation to REA is to calculate it in situ and use corrected σ_w values to make a distinction between updraft and downdraft sampling. That have not been done at Kraków site for the analyzed period, and so the *updraft* and *downdraft* samples were separated with unrotated coordinates. A tilt correction was made for calculation of corrected σ_w values.

Seasonal, diurnal and spatial variability of the CO_2 and CH_4 fluxes during the period of interest were analyzed. The results are presented in Chapter 3.

2.4. Spectral analysis

An example power spectra of anemometer readings are shown in the **Fig. 5**. An unusual temperature power spectrum indicates high contribution of white noise to the instrument reading. This high-frequency end seems to be especially pronounced for large $|L|$ values (approaching neutral stratification).

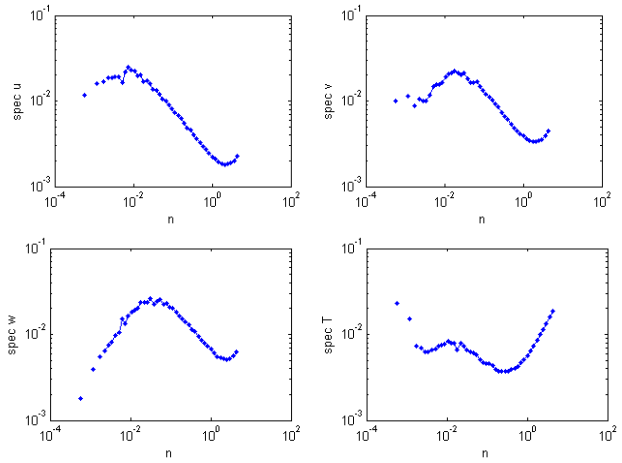

Fig. 5. *Power spectra of the wind* u,v,w *components and sonic temperature* T *for February 2013. Spec(x) stands for a power spectrum normalized with x variance, and n is natural frequency.*

Fig. 6 shows an example cospectra of temperature and wind vertical component for stable and unstable atmosphere stratification along with Kaimal [14] ideal cospectra fit. For unstable atmosphere stratification the cospectrum shape agrees well with the model, but for stable conditions they do not, in both high and low frequency end.

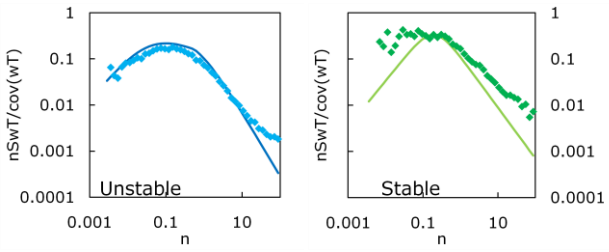

Fig. 6. *Example cospectra of temperature and vertical wind component for unstable and stable stratification. Dots represent calculated values and lines are Kaimal model [14] fits (data from June 2013).*

A spectral analysis was not done entirely during the visit at Helsinki University; it will be performed in the future.

3. Obtained results

A heat and momentum flux quality control for each half-hour in the analyzed period left 25% of all the data marked with the highest quality flag (quality flag 0, [13]). Unless specifically marked, all the flux results presented below are filtered with this condition. As using of a soft quality check (quality flag 1) is allowed for specific implementations, future work includes expanding amount of data using this less reliable dataset.

3.1. Wind statistics

A wind roses for analyzed period is presented in **Fig. 7**. The prevailing wind directions are from west and north-east and are in agreement with the independent wind measurements at the site [15].

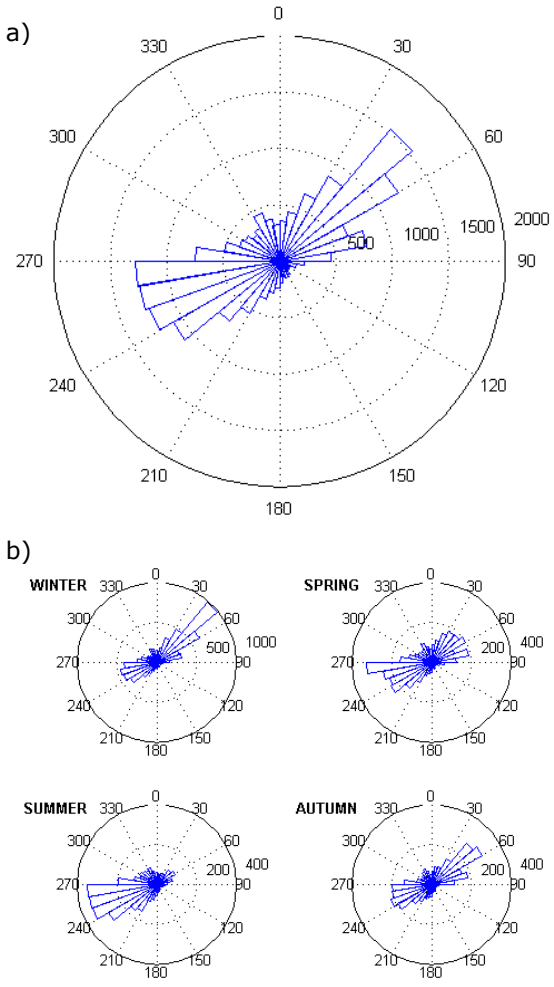

Fig. 7. *a) Wind rose of the analyzed period. b) seasonal wind roses. Radial axis represent number of events in analyzed period.*

Wind direction varied with the season. During summer prevailing wind direction was W, in winter NE. Mean value of the wind speed during analyzed period (July 2012 – March 2014) is 2.2±1.5 m/s, median 2 m/s, 25th and 75th percentiles 1.1 and 3.2 m/s. Seasonal variability of the wind speed is shown in **Fig. 8**.

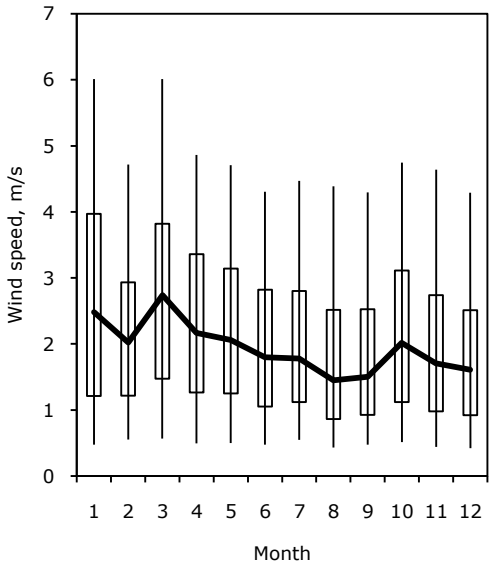

Fig. 8. *Seasonal variability of wind speed at Kraków site.*

Fig. 9 presents calculated friction velocity u_* histograms for unfiltered and quality filtered [13] data. The filtering significantly improved a distribution of friction velocity.

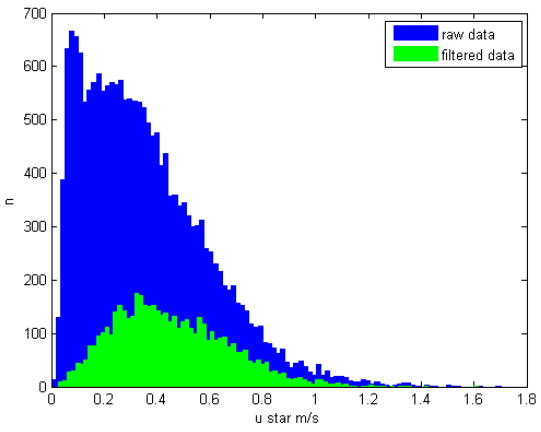

Fig. 9. *Friction velocity histogram for all of the analyzed data (blue) and the high quality data (quality flag =0, green; see* Chapter 2.3*).*

As advised by the hosting institute, five atmosphere stability types were assumed: neutral, very unstable, unstable, very stable and stable, with the Monin-Obukhov length *L* as a separating criterium **(Fig. 10)**. Very rare occurrence of neutral conditions was noted, and as anticipated nighttime stratification was stable in most cases, and daytime – unstable. Very unstable conditions occurred mostly in mornings and evenings.

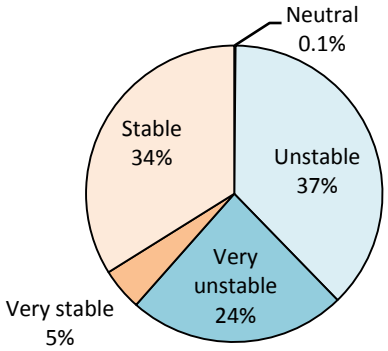

Fig. 10. *Atmosphere stability at Kraków site during the analyzed period.*

3.2. Footprint analysis

Using the data record from Kraków and two seperate models: Kljun [12] and Kormann and Meixner [11], a footprint analysis was performed for each half-hour during the period of interest.

A peak of a footprint function was found at 130m distance from the mast (median value of all the cases), and 90% relative contribution to the flux was found at 350m. As ninety percent of the calculation results were within 430m from the mast, 500m footprint area was established.

Three different types of terrain are to be found in the site surroundings: residential, including buildings and parking lots; streets; a city park and other green areas **(Fig. 11)**. According to the surface cover, four footprint sectors were established. Green sector, located mostly south of the mast, includes the park and a stadium parking. Road sector, north of the mast, includes a busy street. Residential sectors extend east and west from the mast, wherein almost all of the east part within the footprint belong to the university campus. As in a highly heterogeneous urban area it is impossible to make a clear distinction of the sources, borders between the sectors should be considered an approximation.

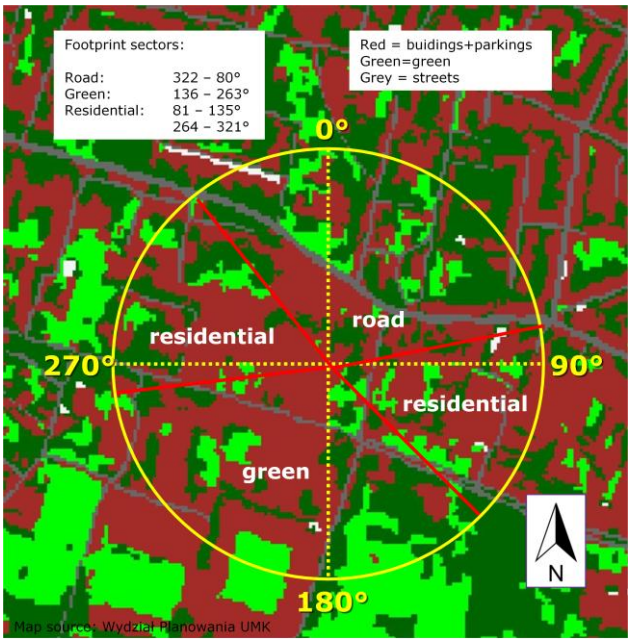

Fig. 11. *Site surroundings with different surface cover types. Averaged footprint and established footprint sectors are also marked.*

3.3. CO_2 fluxes

Seasonal variability of CO_2 flux

All the CO_2 fluxes from the analyzed period are presented in **Fig. 12**. This dataset is already corrected, and questionable period is discarded (Chapter 2.2). Respective plot for methane fluxes can be found in Chapter 3.4 **(Fig. 20)**. Generally, in spring flux values are more spread than in other seasons, due to still used house heating and growing biosphere activity. In summer and autumn fluxes are less variable.

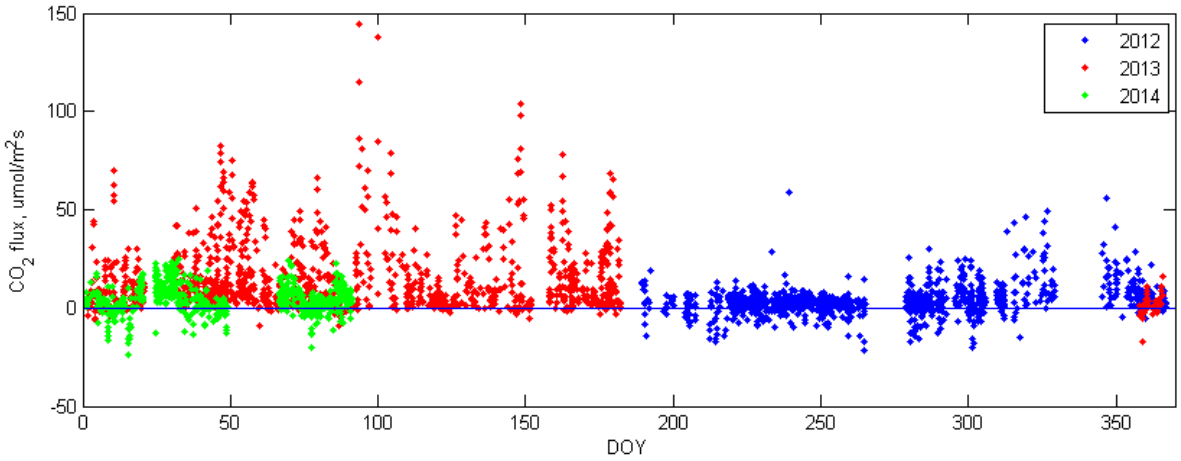

Fig. 12. *CO_2 flux measured at the Kraków site from June 2012 to March 2014.*

Fig. 13 presents seasonal variability of the CO_2 flux. The highest fluxes as well as largest spread were observed in Spring, with the median values around 10 µmol/m^{2}s. The lowest CO_2 flux, with a median below 5 mol/m^{2}s, was found in three summer months: July, August and September. Taking into consideration the similarity in these months in CO_2, as well as CH_4 fluxes lowest values, author decided to change the usual season distinction to make July, August and September one season.

A boxplot in **Fig. 14** shows the seasonal variability of CO_2 flux in Kraków with the alternative seasons.

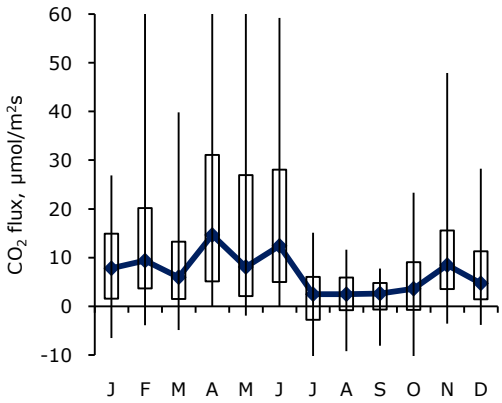

Fig. 13. *Monthly variability of CO_2 flux in Kraków.*

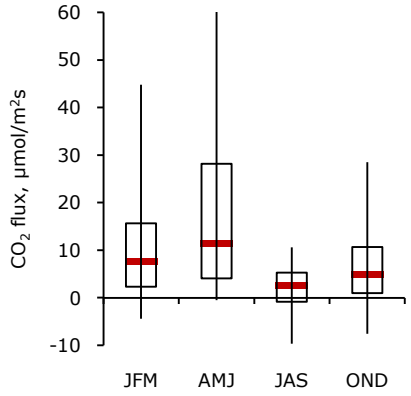

Fig. 14. *Seasonal variability of CO_2 flux in Kraków.*

Obtained CO_2 flux values are higher than previous assessment with a sodar measurements [16]: CO_2 flux varied between 0.6 µmol/m^{2}s in winter and 5.6 µmol/m^{2}s in summer. This difference may be caused by taking into account diurnal variability of CO_2 flux in REA results; in [16] only nighttime fluxes were calculated.

For a comparison, in Florence, Italy measured CO_2 fluxes varied between 7.5 and 10 µmol/m^{2}s (in winter) [3]; in Helsinki CO_2 flux varied between different surface cover sectors and seasons, from −13 µmol/m^{2}s (summer, vegetation sector 25th percentile) reaching 30 µmol/m^{2}s (spring, road sector 95th percentile; [1, *Table 3*].

Spatial variation of CO_2 flux

In general, the highest CO_2 fluxes were observed in the north-east direction. It is also one of the prevailing wind directions (to compare see wind rose, **Fig. 7**). A lot of variability in CO_2 flux is noticed in the park direction (south-east), which indicates very heterogeneous sources and sinks of carbon dioxide **(Fig. 15)**.

Flux spatial distribution vary strongly with the season **(Fig. 16)**. There is strong, apparent assimilation in winter in the city park direction, which can be an indication that the established seasonal division is wrong – winter also includes March. Future work includes a high-resolution spatial and seasonal analysis of the flux along with the atmospheric turbulence characteristics from that direction to find a reason of such unrealistic results.

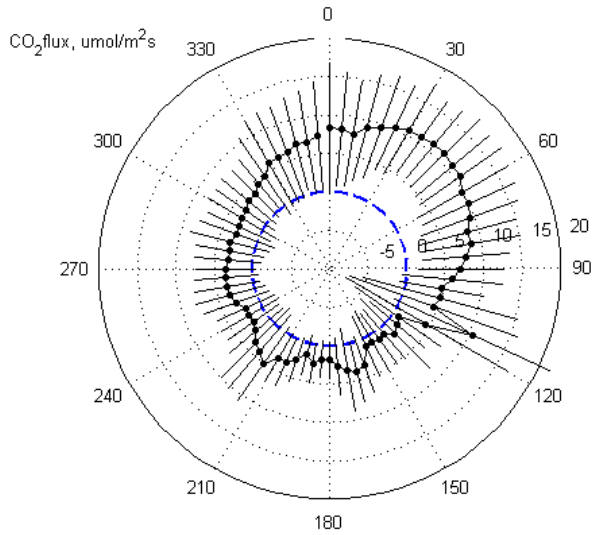

Fig. 15. *CO_2 flux spatial variability. Blue line indicates 0 µmol/m^{2}s.*

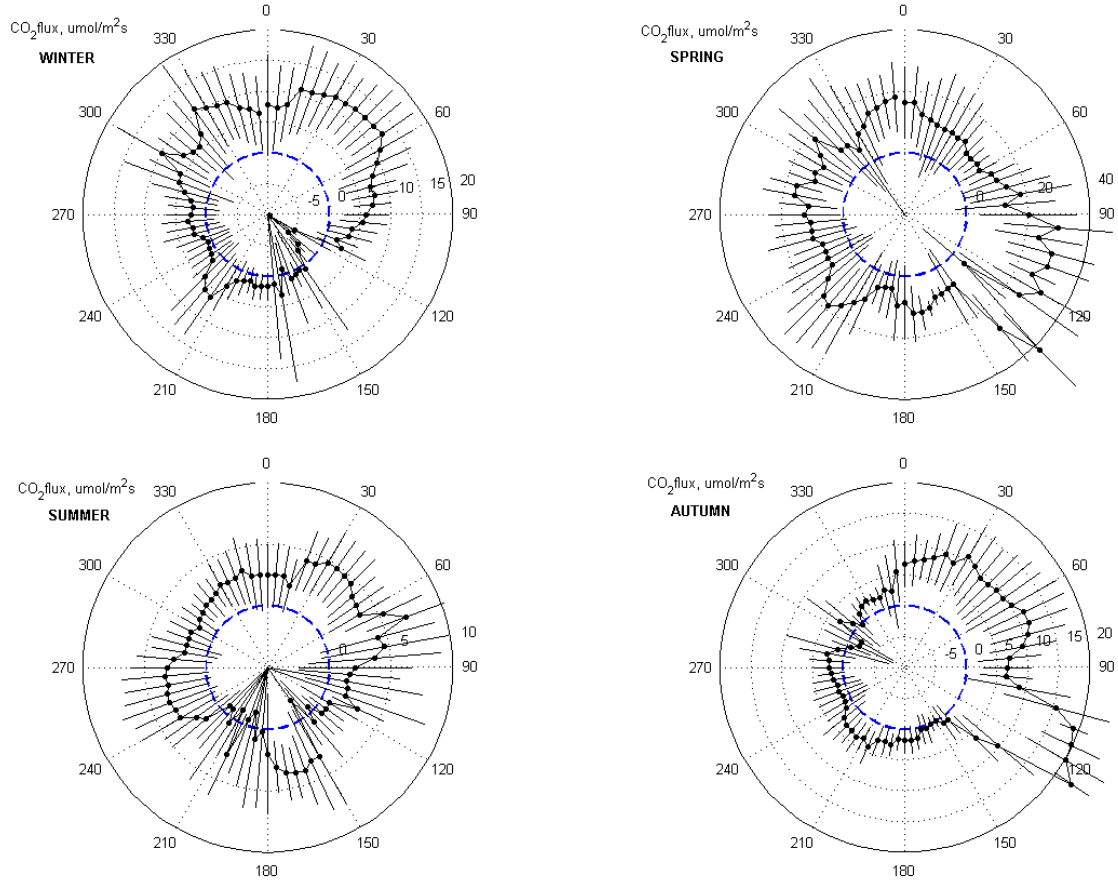

Fig. 16. *Seasonal variability of spatial CO_2 flux distribution in Kraków. Note the different flux axis scales. Blue line indicates 0 µmol/m^{2}s.*

CO_2 fluxes in spring are more evenly distributed with the direction, with an exception of south-east part, where a park is located. In this season the highest emissions are noticed in SE area, instead of NE direction. The same, even more expressive, is visible in autumn. However in this season the flux maximum is shifted more up north in comparison to spring, which may indicate different CO_2 source.

In summer, CO_2 fluxes are in general much smaller than in other seasons, due to assimilating biosphere. In some directions, correlating with location of green areas, a flux median for July, August and September is below zero.

As described in Chapter 3.2, four footprint sectors were established for the site, with three different CO_2 source types: residential, road and green **(Fig. 11)**. 25th, 50th and 75th percentiles of CO_2 flux from these sectors are presented in **Fig. 17**.

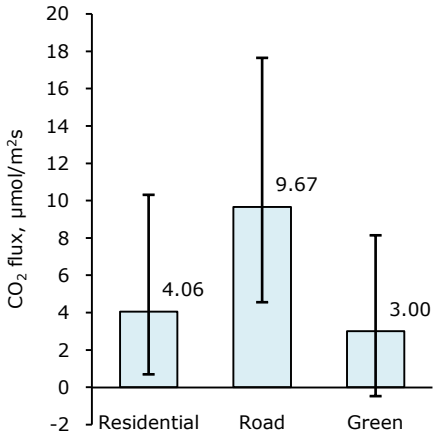

Fig. 17. *CO_2 flux from different source areas.*

The lowest flux is observed in the green sector, with 25th percentile below zero, meaning that in more than 1/4 of the analyzed period (which also included two winters) biosphere was assimilating efficiently enough to absorb more CO_2 than it was emitting.

The highest CO_2 fluxes were observed in the road sector north of site, which includes a busy street and an often jammed intersection. More throughout footprint analysis should reveal whether the source of CO_2 is traffic or residential buildings, which are located further away from the measurement mast in this direction.

Diurnal variability of CO_2 flux

Mean diurnal variability of CO_2 flux observed in Kraków during the analyzed period is shown in **Fig.18**. Again, in spring the fluxes are noticeably higher than in other seasons, with maximum around midday. CO_2 fluxes are the lowest in summer, reaching negative values around noon and maximum after the sunset. In winter, two peaks are noticeable during the day, which, in the absence of biosphere, can be related to rush hours. In autumn, higher CO_2 fluxes are observed in the afternoon than in the morning but diurnal variability is not as clear as in other seasons.

Respective plots for different footprint sectors are shown in **Fig. 19**. Residential sector is most heterogeneous, and so is the diurnal variability of the flux. Daytime CO_2 fluxes are higher than during the night, with an exception of summer, when assimilation by the biosphere is most efficient. In road sector a pattern of two rush hours peaks is visible in all seasons with an exception of spring. Very low CO_2 fluxes are measured in the green sector, with some negative mid-day values observed also in autumn.

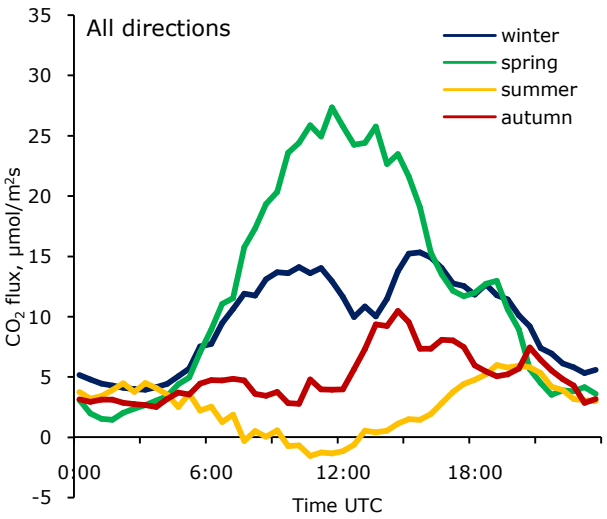

Fig. 18. *Mean diurnal variability of CO_2 flux in all seasons (two-hour running mean).*

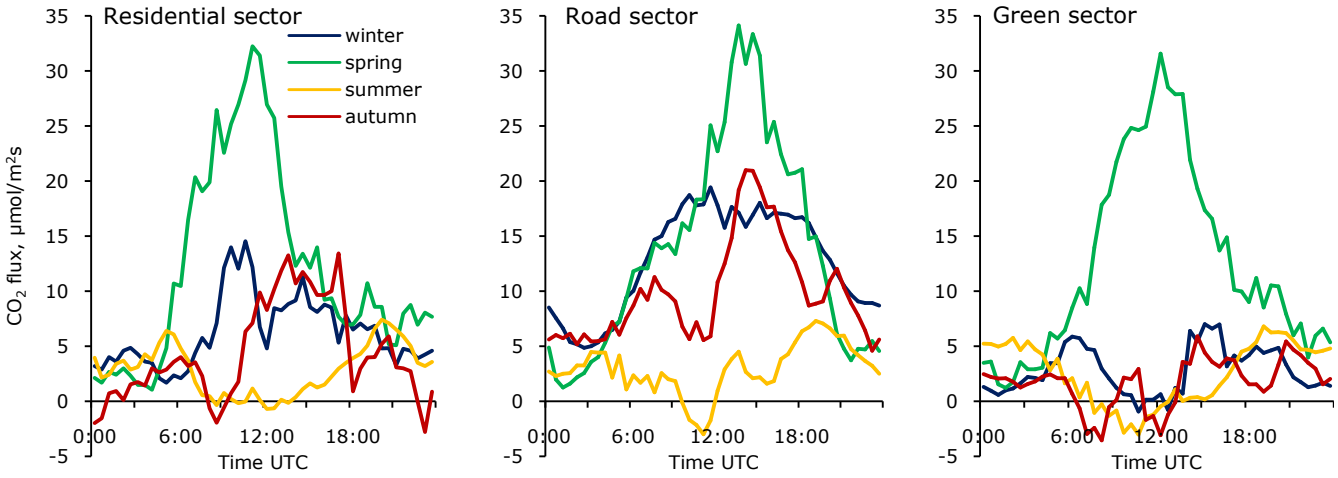

Fig. 19. *Mean diurnal variability of CO_2 flux in all seasons for residential, road and green sectors (two-hour running mean).*

3.4. CH_4 fluxes

Seasonal variability of CH_4 flux

CH_4 fluxe dataset is shown in **Fig 20**. These data are to be considered with caution because of uncertain CH_4 concentration measurement. Some general patterns can be extracted from existing dataset, however for a throughout analysis of CH_4 fluxes, filtering of uncertain concentration measurement will be done in the future. A period from July to December 2013 is not taken into account due to possible measurement system malfunction (see Chapter 2.2.).

Measured methane fluxes are more variable than CO_2. No apparent seasonality is to be seen with raw data, however in summer there are less negative fluxes. Single events of very high positive and negative fluxes were observed.

CH_4 flux seasonal variability is shown in **Fig. 21** and **Fig. 22**.

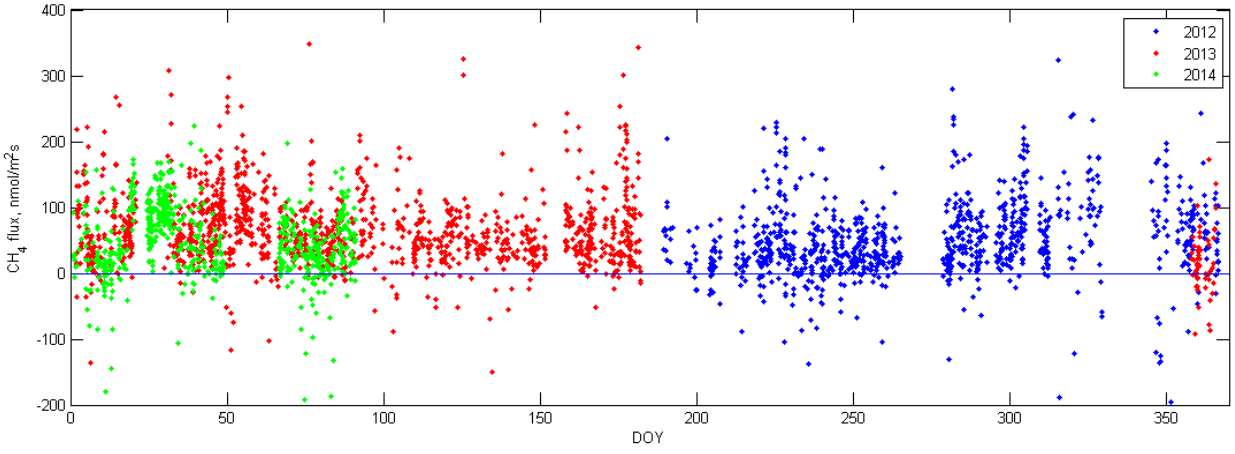

Fig. 20. *CH_4 flux measured at the Kraków site from June 2012 to March 2014.*

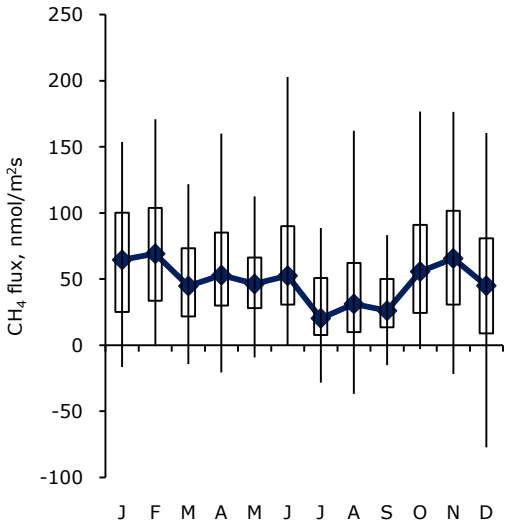

Fig. 21. *Monthly variability of CH_4 flux in Kraków.*

Seasonal changes of CH_4 flux are visible in median values, following CO_2 flux seasonal pattern (compare to **Fig.13** and **Fig. 14**). The highest fluxes were observed in winter and autumn, the lowest in summer. The same season distinction is applied as in the CO_2 flux analysis.

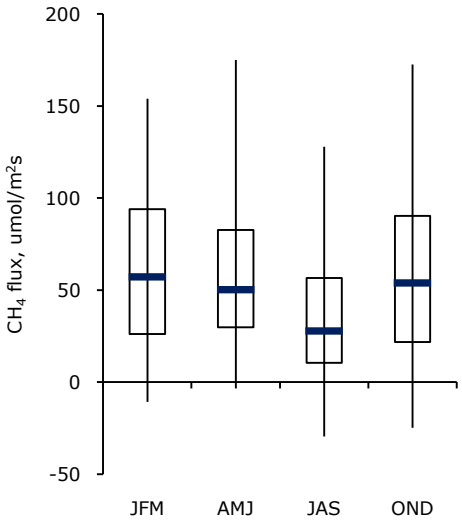

Fig. 22. *Seasonal variability of CH_4 flux in Kraków.*

Yearly median CH_4 flux for analyzed period is 49.1 nmol/m^{2}s (21.8 – 85.6, 25th and 75th percentile, respectively). This is consistent result with other CH_4 urban flux measurements: in Florence, Italy, measured CH_4 flux varied between around 90 and 180 nmol/m^{2}s [3].

Spatial variation of CH_4 flux

The highest values of CH_4 flux were observed in north-east direction from the mast, the same as for the CO_2 fluxes (**Fig. 23**, to compare with **Fig. 15**). A peak in CH_4 flux is visible in 310° direction. Previous research (CH_4 plume hunting, not published) revealed elevated CH_4 concentration in that direction, however it was located ca. 2 km from the site, so that source should not be included in the footprint.

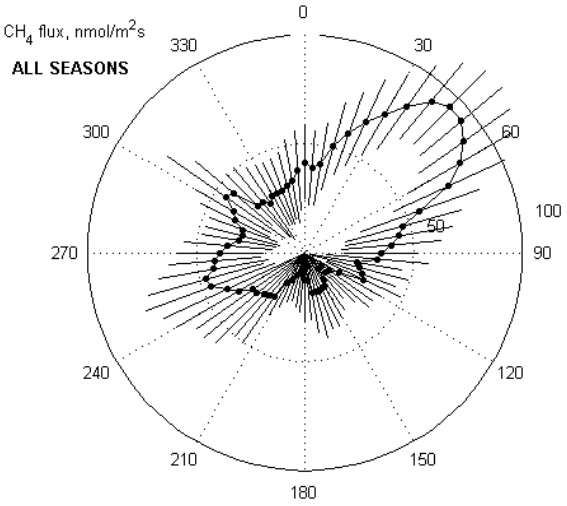

Fig. 23. *CH_4 flux spatial variability.*

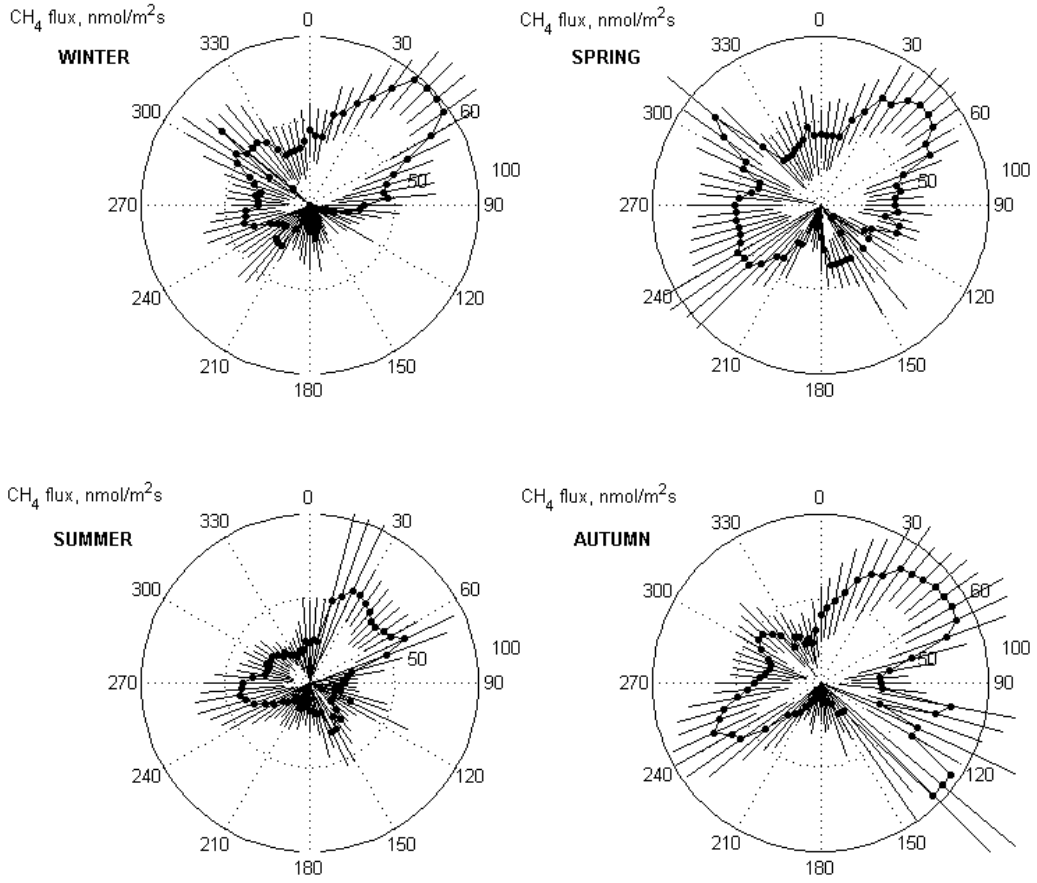

Fig. 16. *Seasonal variability of spatial CH_4 flux distribution in Kraków.*

High CH_4 flux in north-west direction is present in all of the seasons. Mentioned previously flux peak at 310° is observed in all seasons except of summer, especially visible in spring; in winter elevated flux region in that direction is wider, as if the emitted gas was horizontally dispersed because of more frequent and prolonged atmospheric inversions in that season.

Most variable fluxes were observed in the south-west direction. In winter, at 140°, there was a negative value observed; in contrast, in autumn in almost the same direction a very large flux was found. Until additional filtering of the data mentioned in the beginning of this chapter is done, no conclusion should be drawn on such flux variability.

The 25th, 50th and 75th percentiles of CH_4 flux in the footprint sectors are presented in **Fig. 25**. As in CO_2 case, CH_4 fluxes from the road sector located north of the site are higher than in green and residential sectors.

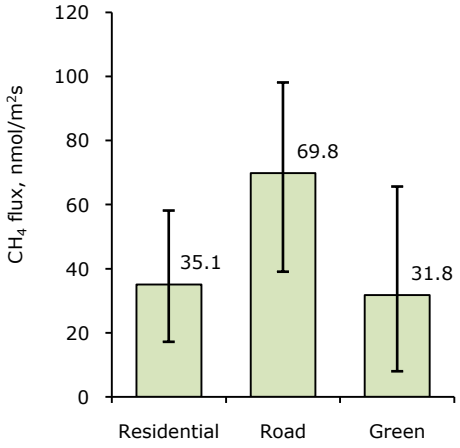

Fig. 25. *CH_4 flux from different source areas.*

Diurnal variability of CH_4 flux

Mean diurnal variability of CH_4 flux in Kraków is shown in **Fig. 26**. In summer, CH_4 flux remains approximately constant whole day, varying between 30 and 40 nmol/m^{2}s. In other seasons clear diurnal pattern is visible, however it looks differently for each season. A morning peak is noticeable around 09:00 UTC, then CH_4 flux decreases. In spring, minimum flux is present after sunset to increase gradually during the night; in autumn, after late afternoon minimum the flux increases to reach second peak in the evening; in winter the flux lowest values are observed during the night and just after the mid-day peak, after which a second increase in the flux is present.

Respective plots for different footprint sectors are shown in **Fig. 27**.

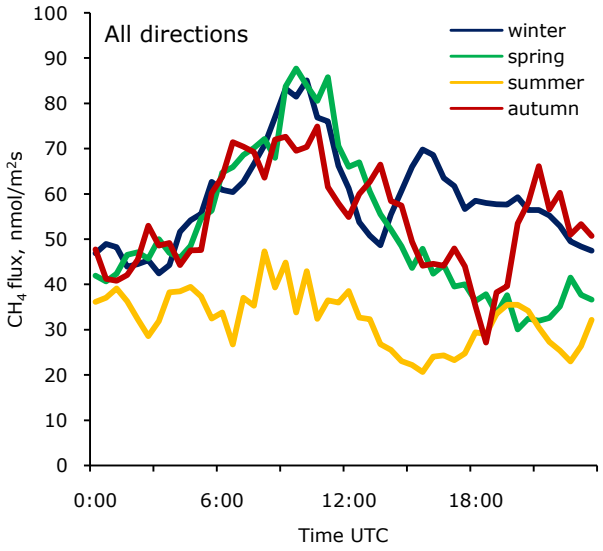

Fig. 26. *Mean diurnal variability of CH_4 flux in all seasons (two-hour running mean).*

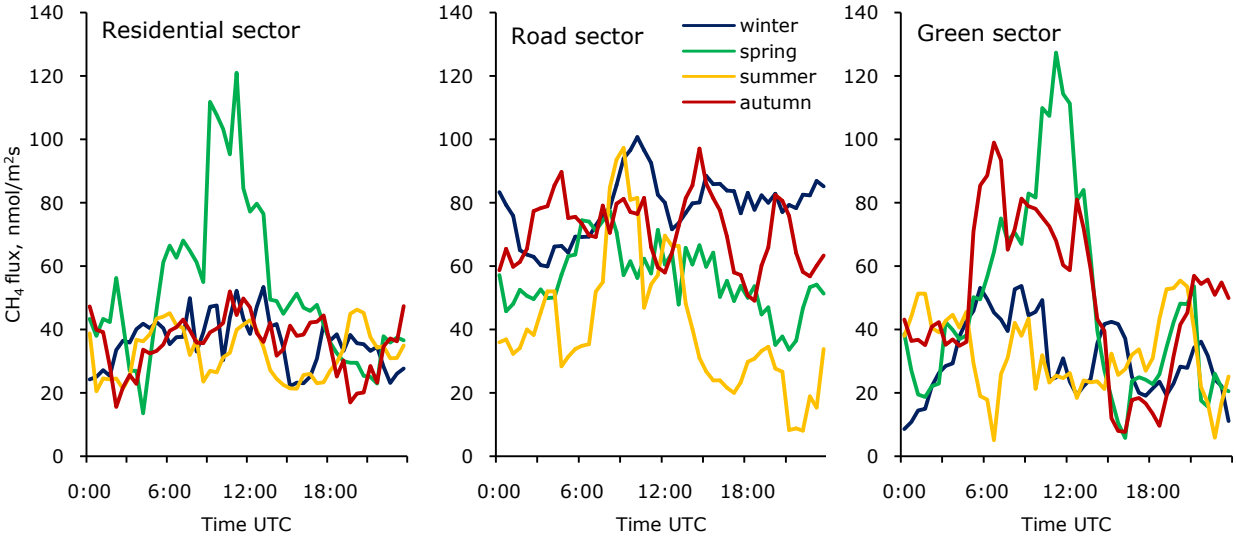

Fig. 27. *Mean diurnal variability of CH_4 flux in all seasons for residential, road and green sectors (two-hour running mean).*

In the road footprint section, diurnal flux variability is not clear in all seasons but summer, however in most part of the year a morning peak is distinguishable. Winter CH_4 fluxes in this sector are higher than in other seasons.

In the residential sector, in all seasons, daytime CH_4 fluxes are higher than during the night. This diurnal pattern is especially evident in spring, when peak CH_4 flux is almost three times over the nighttime average.

In the green sector clear diurnal variability of the CH_4 flux is present in spring and autumn: an increase in the morning and a rapid decrease after reaching a peak value.

To explain both spatial and temporal variability of CH_4 flux measured in Kraków, location of nearby methane

sources is needed. Anthropogenic sources include possible city gas network leakages, leaking stoves in neighboring residential buildings, sewage system and trash containers.

4. Future work

During three months visit author gained an extensive knowledge of handling with micrometeorological data, and got several useful data analysis tools. However, it was not enough amount of time to do the entire two-year dataset analysis. Future work with Kraków REA dataset includes:

- throughout analysis of power spectra and cospectra of the sonic data,
- assessment of the half-year long data record that have been discarded in this study due to possible REA measurement system malfunction,
- sensible heat fluxes analysis,
- applying additional filtering of CH_4 flux data, related to precision of concentration measurement,
- gap filling of discarded flux values,
- comparison of calculated fluxes of CO_2, CH_4 and sensible heat with slow-changing meteorological data, such as temperature, precipitation or radiative balance components,
- calculating spatial and temporal variability of CO_2 and CH_4 fluxes for a dataset extended by low quality results [13].

Some parts of work that have been done during the visit at Helsinki University will be presented at the *First International ICOS Science Conference* in Brussels, 23-25 September 2014. A publication comparing REA CO_2 flux results with chamber measurements in Kraków [5] is planned. A comparison between Kraków and Helsinki CO_2 and CH_4 fluxes have not been done during the visit as it was planned.

Analysis of CO_2 fluxes measured at Kraków REA site will be an important part of author's PhD thesis.

5. Other activities

During twelve weeks visit at the Helsinki University author took part in the Atmospheric Physics group activities, such as PhD thesis defenses or weekly division seminars, from which general knowledge of aerosols measurements and weather modeling have been gained. Author attended *Global Biogeochemical Cycles* academic course given by Professor Martin Heimann, which was a valuable source of knowledge concerning Earth's climate and its driving forces. Author was assigned to organize early career scientists meeting at the ICOS Science Conference in Brussels, September 2014. Author also took part in 3rd ICOS-Finland Science Workshop in Kuopio, 26-28 May 2014 and visited Hyytiälä forestry station, where chamber comparison campaign for N_2O fluxes was taking place. An important part of author's PhD thesis is based on CO_2 chamber flux measurements; the chamber that was used in Kraków for flux measurements also takes part in this campaign.

Fig. 28. *The visit at Helsinki University was also an opportunity to admire rare atmospheric phenomena such as halo (picture taken at the university campus, 14 May 2014).*

6. References

[1] Vesala T., Järvi L., Launiainen S. et al., 2008. Surface-atmosphere interactions over complex urban terrain in Helsinki, Finland. Tellus 60B, 188-199.

[2] Pawlak W., Fortuniak K., Siedlecki M., 2011. Carbon dioxide flux in the centre of Łódź, Poland – analysis of a 2-year eddy covariance measurement data set. International Journal of Climatology 31, 232-243.

[3] Gioli B., Toscano P., Zaldei A., Fratini G., Miglietta F., 2013. CO_2, CH_4 and particles flux measurement in Florence, Italy. Energy Procedia 40, 537-544.

[4] Velasco E., Pressley S., Allwine E., Westberg H., Lamb B., 2005. Measurements of CO_2 fluxes from the Mexico City urban landscape. Atmospheric Environment 39, 7433–7446.

[5] Jasek A., Zimnoch M., Gorczyca Z. et al., 2014. Seasonal variability of soil CO_2 flux and its carbon isotope composition in Krakow urban area, Southern Poland. Isotopes Environ. Health Stud. Epub 2014 Jan 20. DOI: 10.1080/10256016.2014.868455.

[6] Zimnoch M., Jelen D., Galkowski M. et al., 2012. Partitioning of atmospheric carbon dioxide over Central Europe: insights from combined measurements of CO_2 mixing ratios and their isotopic composition. Isotopes Environ. Health Stud. 48(3), 421-33.

[7] Zimnoch M., 2009. Stable isotope composition of carbon dioxide emitted from anthropogenic sources in the Krakow region, Southern Poland. Nukleonika 56(4), 291-295.

[8] Ammann C., Meixner F.X., 2002. Stability dependence of the relaxed eddy accumulation coefficient for various scalar quantities. Journal of Geophysical Research 107 (D8),10.1029/2001JD000649.

[9] Wieringa J., 1980. Representativeness of wind observations at airports. Bulletin of the American Meteorological Society, 6 1 , 962–971.

[10] Hsieh C. I., Katul G., Chi T. W., 2000. An approximate analytical model for footprint estimation of scalar fluxes in thermally stratified atmospheric flows. Advances in Water Resources 23, 765-772.

[11] Kormann R., Meixner F.X., 2001. Analytical footprint model for non-neutral stratification. Boundary-Layer Meteorology 99, 207-224.

[12] Kljun N., Calanca P., Rotach M.W., Schmid H.P., 2004. A simple parameterization for flux footprint predictions. Boundary-Layer Meteorology 112, 503-523. Online footprint calculation: *http://footprint.kljun.net/*.

[13] Mauder M. and Foken T., 2004. Documentation and instruction manual of the eddy covariance software package TK2, Universitat Bayreuth, Abt. Mikrometeorologie, Print, ISSN 1614-8916, Arbeitsergebnisse, 26, 44 pp.

[14] Kaimal J. C., Wyngaard J. C., Izumi Y. , Cote O.R., 1972. Spectral Characteristics of Surface-Layer Turbulence, Quart. J. Roy. Meteorol. Soc. 98, 563–589.

[15] Meteo station at AGH-UST, *http://meteo.ftj.agh.edu.pl/meteo/*.

[16] Zimnoch M., Godlowska J., Necki J. et al., 2010. Assessing surface fluxes of CO_2 and CH_4 in urban environment: a reconnaissance study in Krakow, Southern Poland. Tellus 62B, 573-580.